Chapter 3

Rheology and Ultrasonic Properties of $Pt_{57.5}Ni_{5.3}Cu_{14.7}P_{22.5}$ Liquid

Key words: Bulk metallic glass, Non-Newtonian flow, Liquid fragility, Ultrasonic measurement, Compression test, Amorphous

3.1 Abstract

The equilibrium and non-equilibrium viscosity and isoconfigurational shear modulus of $Pt_{57.5}Ni_{5.3}Cu_{14.7}P_{22.5}$ supercooled liquid are evaluated using continuous-strain-rate compression experiments and ultrasonic measurements. By means of a thermodynamically consistent cooperative shear model, variations in viscosity with both temperature and strain rate are uniquely correlated to variations in isoconfigurational shear modulus, which leads to an accurate prediction of the liquid fragility and to a good description of the liquid strain rate sensitivity.

3.2 Introduction

The Pt-Ni-Cu-P bulk-glass forming system [1] is known to form one of the toughest bulk metallic glasses to date [2-4], characterized by a fracture toughness value of ~ 80 MPa-$m^{1/2}$. The inherent toughness of this system is shown to be a consequence of its tendency to undergo extensive shear-band networking prior to fracture [2]. This tendency has been primarily attributed to its high Poisson's ratio (~ 0.42), which designates that the material favors accommodation of stress by shear. Interestingly, Poisson's ratios of metallic glasses were recently shown to be directly correlated to the rheology of their undercooled liquid state, and specifically to the liquid fragility [5]. In a recent rheological study [6] it was demonstrated that Pt-based liquid is indeed one of the most fragile metallic-glass-forming liquids, which to some extent explains its inherently tough nature. In the present study we employ continuous-strain-rate compression experiments and acoustic measurements in conjunction with a recently developed cooperative shear model [7-9] to assess the rheology and ultrasonic properties of $Pt_{57.5}Ni_{5.3}Cu_{14.7}P_{22.5}$ liquid under equilibrium and non-equilibrium conditions.

3.3 Experimental

The rheology of the supercooled liquid was assessed using the continuous-strain-rate compression setup as described in Ref. [10]. The alloy ingot was prepared by first pre-alloying Pt (99.9mass%), Ni (99.9mass%), and Cu (99.99mass%) by induction melting, and then alloying P (99.999mass%) by step-wise furnace heating. The specimens were prepared by first fluxing the alloy with B_2O_3, and subsequently casting it into 4 mm diameter rods, whose amorphous nature was verified by thermal analysis. The rods were cut and polished to form 4 mm tall cylindrical specimens. The typical 2-to-1 geometric ratio was not adopted here, as the 1-to-1 ratio was found more appropriate in geometrically constraining the specimen against excessive barreling (possibly related to a high Poisson's ratio). The compression experiments were performed for at least 5 Maxwellian relaxation times after the transient stress strain response to ensure that a steady-state flow stress was attained. The strain-rate dependent viscosity was measured at temperatures ranging from 473 K to 523 K, and is presented in Fig. 1. The strain-rate dependence exhibits the typical trend observed in other glass forming systems: in the low strain rate limit, viscosity is stabilized at the Newtonian limit characterized by a strain-rate sensitivity exponent of 1.0; In the high strain rate limit, viscosity is stabilized at a non-Newtonian limit characterized by a strain-rate sensitivity exponent of ~ 0.1.

The isoconfigurational shear modulus at the high-frequency "solid-like" limit was evaluated using ultrasonic measurements along with density measurements [11]. Ultrasonic shear wave speeds were measured using the pulse-echo overlap set-up described in Ref. [8]. Densities were measured by the Archimedes method, as given in the American Society for Testing and Materials standard C693-93. Measurements were

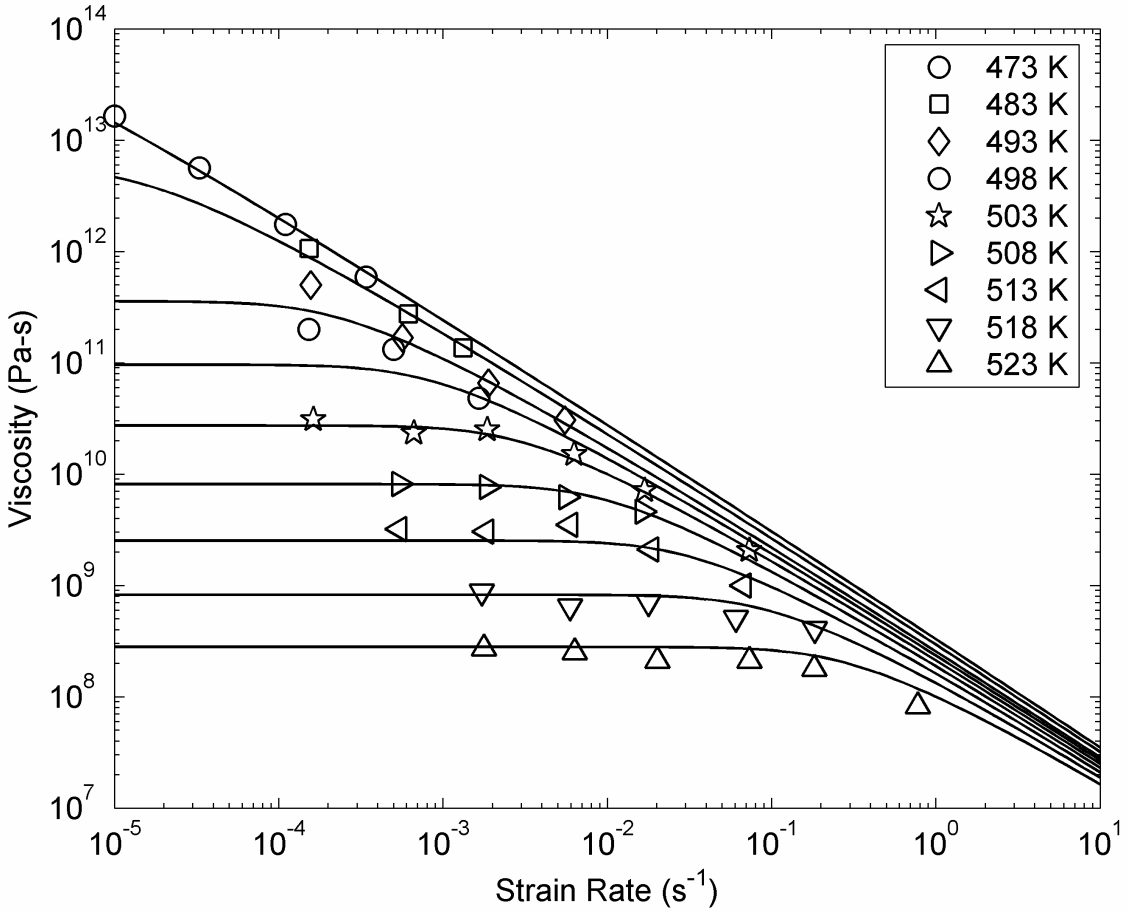

Figure 3.1. Viscosity of $Pt_{57.5}Ni_{5.3}Cu_{14.7}P_{22.5}$ at the indicated temperatures and strain rates assessed from continuous–strain-rate compression experiments. Lines are fits to the data using the kinetic balance formulation given in Eq. (3.4).

performed *ex situ* on the amorphous specimens at room temperature, after being quenched rapidly from the processing temperature. The isoconfigurational shear moduli at the processing temperatures were estimated by extrapolating the room temperature measurements using a linear Debye-Grüneisen constant to account for the thermal expansion effect on the shear modulus of the frozen glass. A measured linear Debye-Grüneisen coefficient of ~ 13 MPa/K for $Pt_{57.5}Ni_{5.3}Cu_{14.7}P_{22.5}$ was utilized [12]. We measured the temperature-dependent equilibrium isoconfigurational shear modulus by performing ultrasonic measurements on relaxed undeformed specimens annealed at temperatures between 472 K and 503 K**.** We also measured the strain-rate dependent non-equilibrium isoconfigurational shear modulus by performing ultrasonic measurements on specimens deformed at 473 K and strain-rates between 1×10^{-5} and 3.4×10^{-4} s^{-1}. The thermal annealing process, as well as the steady-state deformation process, was performed for several Maxwellian relaxation times to ensure that a steady configurational state had been attained, while the succeeding quenching process was performed as rapidly as possible in order to freeze that configurational state. The results for the ultrasonically measured shear modulus, corrected for the Debye-Grüneisen effect, are presented in Fig. 3.2 for the equilibrium liquid annealed at the indicated temperatures, and in Fig. 3.3 for the non-equilibrium liquid deformed at the indicated rates.

For a more complete description of the experimental methods used in this chapter, please refer to the experimental section in Chapter 2.3.

3.4 Discussion

In several recent studies [7-9], a thermodynamic link between the isoconfigurational shear modulus G and viscosity η has been proposed, as follows:

$$\frac{G}{G_g} = \left[\frac{T}{T_g} \frac{\ln\left(\eta/\eta_\infty\right)}{\ln\left(\eta_g/\eta_\infty\right)} \right]^q \tag{3.1}$$

where T_g is the glass transition temperature, $\eta_g \equiv 10^{12}$ Pa-s is the equilibrium viscosity at T_g, G_g is the equilibrium shear modulus at T_g, and η_∞ is the Born limit of viscosity. The exponent q is defined in previous studies as $q = n/(n+p)$, where n and p are the reduced "elastic" and "cooperative volume" fragility indices, respectively; this quantifies the contributions of isoconfigurational shear modulus and cooperative shear volume to the softening of the shear flow barrier. In a similar analysis for the Zr-based bulk-glass forming liquid [8] it was determined that the best correlation between G and η is obtained when $n \cong p$ (i.e., $q \cong 1/2$). In the present analysis we take $q = 1/2$ to hold for the $Pt_{57.5}Ni_{5.3}Cu_{14.7}P_{22.5}$ liquid as well. For this liquid we also take $T_g = 489$ K (interpolated value for which $\eta_g \equiv 10^{12}$ Pa-s), $G_g = 30.5$ GPa (interpolated value at T_g), and $\eta_\infty \equiv 4.55 \times 10^{-5}$ Pa-s (taken as the Planck's limit of viscosity). We can therefore use Eq. (3.1) to correlate the liquid viscosity evaluated from mechanical tests to the liquid shear modulus evaluated acoustically. In Fig. 3.2 we superimpose the equilibrium shear moduli predicted from Newtonian viscosities, while in Fig. 3.3 we superimpose the

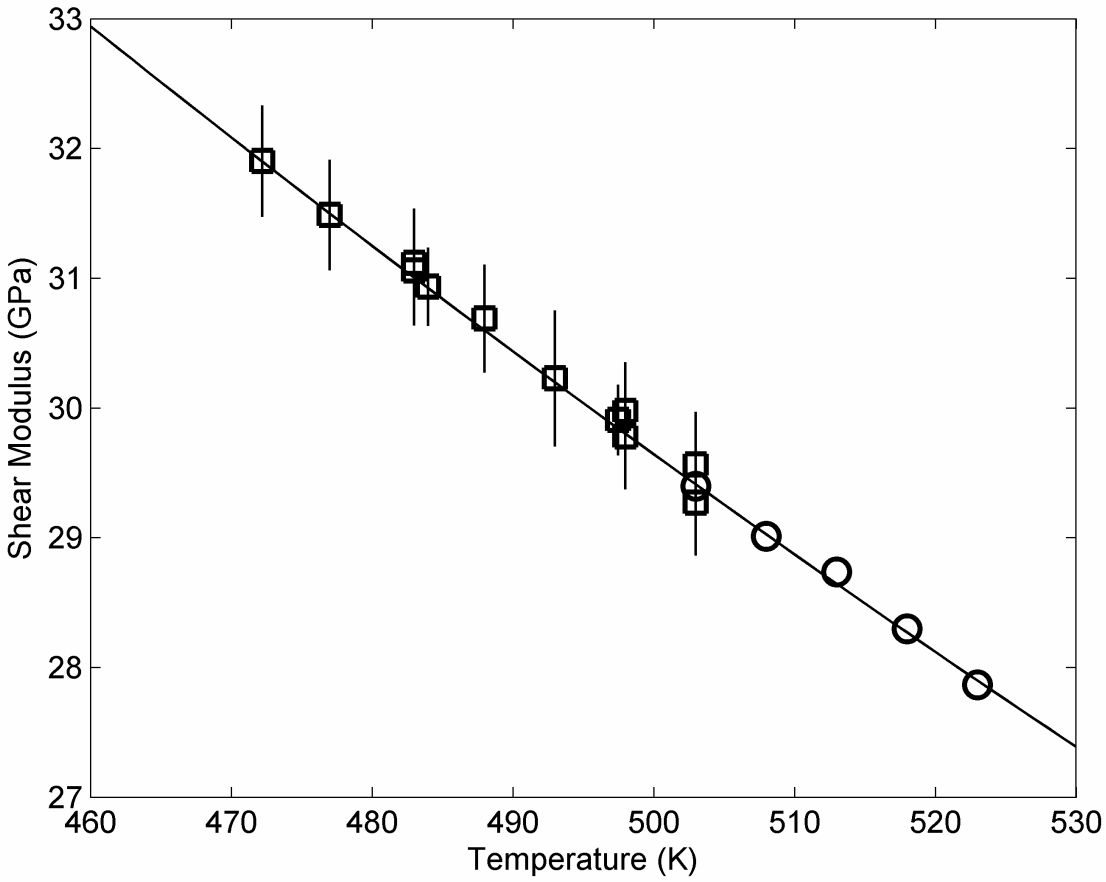

Figure 3.2. Acoustically measured shear modulus corrected for the Debye-Grüneisen effect of the relaxed equilibrium liquid annealed at the indicated temperatures (□). Predicted equilibrium shear modulus from measured equilibrium viscosity data using Eq. (3.2) (○). The line is a fit to the data using the temperature dependence relationship given in Eq. (3.2).

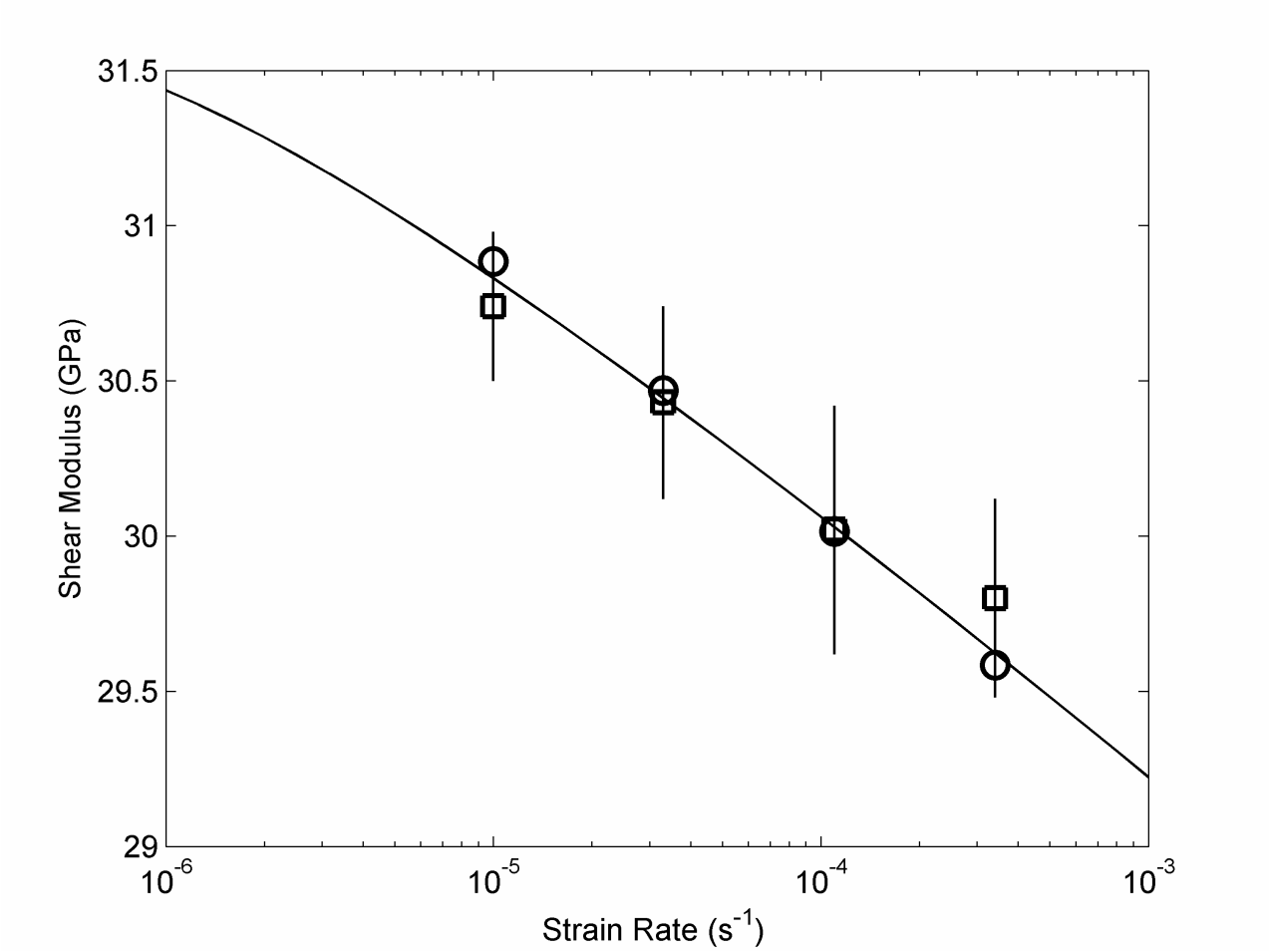

Figure 3.3. Acoustically measured shear modulus corrected for the Debye-Grüneisen effect of the non-equilibrium liquid deformed at 473 K at the indicated strain rates (□). Predicted non-equilibrium shear modulus from measured non-equilibrium viscosity data using Eq. (3.2) (○). The line is a fit to the data using the kinetic balance formulation given in Eq. (3.4).

non-equilibrium shear moduli predicted from non-Newtonian viscosities. As evidenced from these plots, the liquid viscosity can be very well correlated to shear modulus via Eq. (3.1).

A proposed thermodynamic relation for the temperature dependence of the equilibrium isoconfigurational shear modulus, $G_e(T)$, can be utilized to fit the experimental data of Fig. 3.2 and determine the reduced elastic fragility index n for this liquid [9]. This relation is given by:

$$G_e(T) = G_g \exp\left[n\left(1 - T/T_g\right)\right]. \tag{3.2}$$

A fit to the equilibrium data of Fig. 3.2 yields $n = 1.29$. Such a high value for the reduced elastic fragility places $Pt_{57.5}Ni_{5.3}Cu_{14.7}P_{22.5}$ among the most fragile liquids investigated using this treatment [8, 9]. Specifically, the Angell fragility m can be estimated by relating m to n using $m = \left(1 + n/q\right)\log\left(\eta_g/\eta_\infty\right)$ [8], which gives $m = 59$, a value consistent with the fragilities reported previously for similar Pt-based liquids [6].

In the context of this analysis, non-Newtonian flow has been treated as a steady non-equilibrium flow state arising from a balance between the rate of mechanical work and the rate of barrier crossing [9]. The barrier energy density W can be related to η and G as follows:

$$W = kT\ln\left(\eta/\eta_\infty\right) = W_g\left(\frac{G}{G_g}\right)^{1/q} \tag{3.3}$$

where $W_g = kT_g \ln\left(\eta_g / \eta_\infty\right)$ is the equilibrium barrier energy density at T_g. The kinetic balance that determines the non-Newtonian flow state is given by [8]:

$$-\alpha \frac{(n/q)W_g}{T_g \Delta c_p} \eta \dot{\gamma}^2 = \frac{\left(W - W_e\right)\left(W/W_g\right)^q}{\eta / G_g} \tag{3.4}$$

where $\dot{\gamma}$ is strain rate, Δc_p is the specific heat capacity change at T_g, $W_e(T) = W_g \exp\left[(n/q)\left(1 - T/T_g\right)\right]$ is the equilibrium barrier energy density, and α is a model parameter. This parameter arises from treating the irreversible barrier crossing events as uni-molecular Maxwellian relaxation processes, and in essence quantifies the deviation from that assumption. For $Pt_{57.5}Ni_{5.3}Cu_{14.7}P_{22.5}$, the measured $\Delta c_p = 2.56$ MJ/m^3 can be employed [13]. The quantity Δc_p was estimated as the change in specific heat evaluated at the calorimetric glass transition temperature as measured using a Differential Scanning Calorimetry (DSC) trace. Fig. 3.4 presents the DSC trace used for this estimate. As shown in Figs. 3.1 and 3.3, Eq (3.4) is capable of capturing the non-equilibrium viscosity and shear modulus reasonably well over the entire range of strain rates considered, for a parameter value of $\alpha = 38.3$.

For a more detailed description of the model used here please see Chapter 2.4.

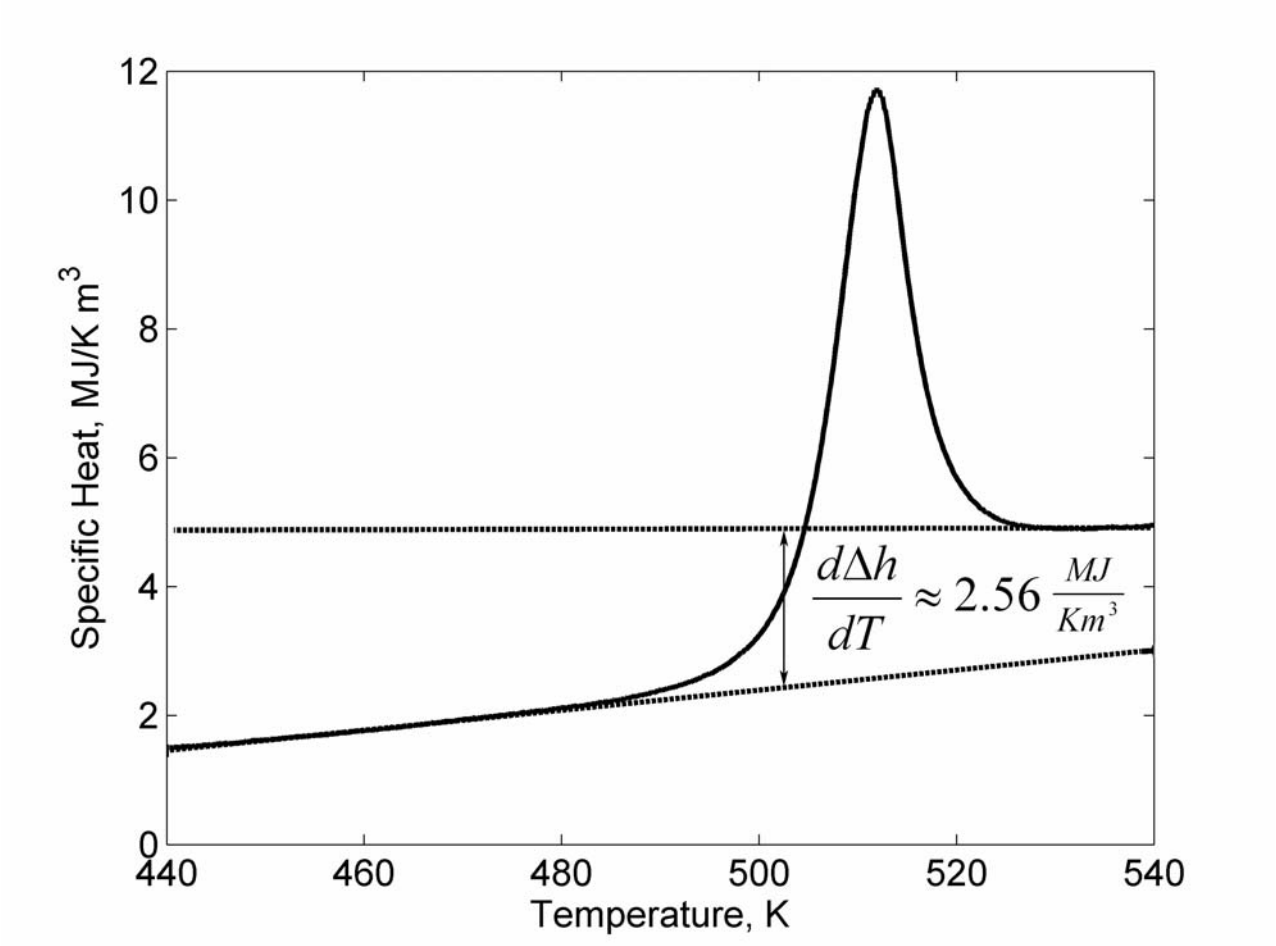

Figure 3.4. The DSC trace used to measure $d\Delta h/dT$ for $Pt_{57.2}Ni_{5.3}Cu_{14.7}P_{22.5.}$

3.5 Conclusion

In conclusion, by means of continuous-strain-rate compression experiments and ultrasonic measurements we evaluated the equilibrium and non-equilibrium viscosity and isoconfigurational shear modulus of $Pt_{57.5}Ni_{5.3}Cu_{14.7}P_{22.5}$ supercooled liquid. By utilizing a thermodynamically-consistent cooperative shear model, we correlated the variations in viscosity with both temperature and strain rate to the variations in isoconfigurational shear modulus, which led to an accurate prediction of the liquid fragility and to a good description of the liquid strain-rate sensitivity.

$Pt_{57.5}Ni_{5.3}Cu_{14.7}P_{22.5}$ is the most fragile metallic glass system that has been fit with the model fully derived in Chapter 2. With these experiments it has been shown that this model is capable of fitting metallic glass systems regardless of how fragile they are. Therefore, it would appear that this theory adequately describes the behavior of metallic glasses and may possibly be applied to other simple liquids. Additional work will be required to extend this theory to polymers or liquids containing more complex interactions. This is due to the change in the potential energy landscape associated with those materials, as well as issues regarding entanglement, cross linking, and other non-trivial effects.

3.6 References

[1] J Schroers, and W L Johnson, Appl. Phys. Lett. 84, 255506 (2004).

[2] J Schroers, and W L Johnson, Phys. Rev. Lett. 93, 3666 (2004).

[3] J J Lewandowaski, W H Wang, and A L Greer, Phil. Mag. Lett. 85, 77 (2005).

[4] M F Ashby, and A L Greer, Scripta Mater. 54, 321 (2006).

[5] G P Johari, Phil. Mag. 86, 1567 (2006).

[6] H Kato, T Wada, M Hasegawa, J Saida, A Inoue, and H S Chen, Scripta Mater. 54, 2023 (2006).

[7] W. L. Johnson, and K. Samwer, Phys Rev. Lett. 95, 195501 (2005).

[8] M. L. Lind, G. Duan, and W. L. Johnson, Phys. Rev. Lett. 97, 015501 (2006).

[9] M D Demetriou, J S Harmon, M Tao, G Duan, K Samwer, and W L Johnson, Phys. Rev. Lett. 97, 065502 (2006).

[10] J. Lu, G. Ravichandran, and W. L. Johnson, Acta Mater. 51, 3429 (2003).

[11] E. Screiber, O. Anderson, and N. Soga, Elastic Constants and their Measurement, McGraw-Hill (1973).

[12] M L Lind, unpublished.

[13] J S Harmon, M D Demetriou, M Tao, and W L Johnson, Appl. Phys. Lett. 90, 131912 (2007).